

David B. Mechem<sup>1,2</sup> and Yefim L. Kogan<sup>2</sup><sup>1</sup>Coastal Meteorology Research Program<sup>2</sup>Cooperative Institute for Mesoscale Meteorological Studies  
University of Oklahoma, Norman, Oklahoma

## 1. INTRODUCTION\*

Microphysical process rates in numerical weather prediction models are most often computed using grid point values of the prognostic variables. While computationally and conceptually attractive, this practice is attached to an assumption that the entire grid volume is uniformly that value. Recent studies (Cahalan et al. 1994; Kogan 1998; Pincus and Klein 2000) document the existence of a systematic bias in process rates that arises when sub-grid variability is ignored. Accounting for this bias in global climate models (GCM) has been the primary focus of most previous work since GCMs, with their typically coarse grid volumes, would be expected to benefit greatly from a treatment of sub-grid heterogeneity.

Severe bias can also be present at grid spacings as small as 2-3 km. Kogan (1998) used results from a large eddy simulation (LES) model to obtain an estimate of this bias for marine stratocumulus at this scale. Process rates obtained at every cloudy point in the LES domain were averaged and compared with the process rate computed from domain-averaged microphysical quantities. Mesoscale models are beginning to be run at these fine grid spacings, so the calculated bias is relevant because the LES domain is approximately the size of a mesoscale model grid column. Rates calculated at all LES grid point locations and then averaged were 5-20 times larger than those calculated from mean quantities.

This paper describes a simple treatment of sub-grid variability for the autoconversion process that has been implemented in the U. S. Navy Coupled Ocean/Atmosphere Mesoscale Prediction System (COAMPS; Hodur 1997). It is shown that allowing for sub-grid heterogeneity, even in a rudimentary fashion, can have a significant impact on a mesoscale forecast of a coastal stratocumulus cloud system.

## 2. TREATMENT OF SUB-GRID AUTOCONVERSION

The bulk microphysical parameterization of Khairoutdinov and Kogan (2000; hereafter denoted "KK"),

---

\*Corresponding author address: David Mechem,  
Cooperative Institute for Mesoscale Meteorological  
Studies, University of Oklahoma, 100 E. Boyd,  
Room 1110, Norman, OK 73019. Email:  
dmechem@ou.edu

designed to provide a more physically realistic treatment of drizzling stratocumulus, has been implemented into COAMPS. Like the Kessler parameterization, the KK scheme sequesters liquid water into precipitable (drizzle) and nonprecipitable (cloud) categories, but the KK scheme uses an additional partial moment, number concentration. The autoconversion rate has the form

$$R_{auto} = 1350 q_c^{2.47} N_c^{-1.79},$$

where  $q_c$  has units of  $\text{kg kg}^{-1}$  and  $N_c$  has units of  $\text{cm}^{-3}$ . The mean process rate inside the grid is obtained by integrating the process rate over the probability distribution function (PDF) of the variables and is equivalent to the spatial integration of the local process rates inside the grid. For the two moment KK scheme, the average autoconversion rate is

$$\overline{R_{auto}} = \int_0^\infty \int_0^\infty P(q_c, N_c) R(q_c, N_c) dq_c dN_c,$$

where  $P$  is the joint PDF for  $q_c$  and  $N_c$ , and  $R$  is the local rate function above.

The PDFs are unknown and must be assumed. We choose gamma distributions for both PDFs,

$$P_1(q_c) = \left( \frac{\alpha_1}{q_c} \right)^{\alpha_1} \frac{q_c^{\alpha_1-1}}{\Gamma(\alpha_1)} e^{-\left( \frac{\alpha_1 q_c}{q_c} \right)}$$

$$P_2(N_c) = \left( \frac{\alpha_2}{N_c} \right)^{\alpha_2} \frac{N_c^{\alpha_2-1}}{\Gamma(\alpha_2)} e^{-\left( \frac{\alpha_2 N_c}{N_c} \right)},$$

where  $\alpha_1$  and  $\alpha_2$  are the shape parameters for the two distributions. We further assume that the product of the two individual PDFs is a good approximation for the joint PDF.  $R_{auto}$  may now be integrated over  $P_1$  and  $P_2$  to produce the grid volume mean autoconversion. The final expression is complicated, and a better approach is to derive a bias factor (Pincus and Klein 2000),

$$B = \frac{\overline{R_{auto}}}{R_{auto}} - 1,$$

which is dependent only upon the shape parameters of the two distributions:

$$B = \frac{\Gamma(\alpha_1 + 2.47)\Gamma(\alpha_2 - 1.79)}{\alpha_1^{2.47}\Gamma(\alpha_1)\alpha_2^{-1.79}\Gamma(\alpha_2)} - 1.$$

In the derivations, the distribution means,  $\overline{q_c}$  and  $\overline{N_c}$ , are assumed to be represented by the grid point values of those variables. Bias factors are shown in Figure 1. For most parameter combinations shown, the bias is at least unity, corresponding to a doubling of the autoconversion rate. Small bias factors correspond to cases in which the distribution is most peaked, where the values tend to be more uniform. The discontinuity at  $\alpha_2 = 1.79$  is a manifestation of the behavior of the KK scheme as  $N_c$  approaches zero. Smaller values of  $\alpha_2$  produce a more significant lower tail in the distribution of  $N_c$  which, because of the  $N_c^{-1.79}$  term, is responsible for a large bias in the grid volume average autoconversion.

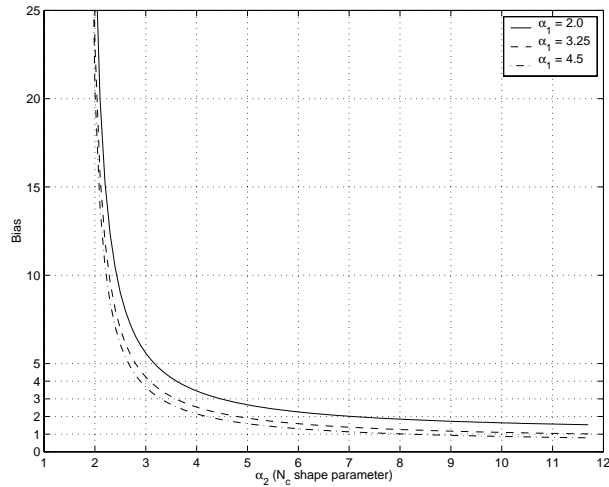


Figure 1. Autoconversion bias for the KK scheme as a function of the  $N_c$  shape parameter ( $\alpha_2$ ) for three different  $q_c$  shape parameters ( $\alpha_1$ ).

The bias is always positive for the KK process rate (as it is for any complex function; see Cahalan et al. 1994). Conceptually, since the KK autoconversion process is proportional to  $q_c^{2.47}$ , sub-grid regions of larger  $q_c$  contribute more to increase the mean autoconversion than regions of smaller  $q_c$  contribute to decrease it. A similar effect is at work for  $N_c$ , with sub-grid regions of low  $N_c$  increasing the mean autoconversion more than regions of high  $N_c$  can reduce it.

In the mesoscale model, the free (shape) parameters  $\alpha_1$  and  $\alpha_2$  are determined from point values of  $q_c$  and  $N_c$ , and are constrained using LES PDFs from broken and solid stratocumulus cloud fields. This makes intuitive sense, to the extent that these two cloud variables are able to independently diagnose cloud fraction and thus which LES distributions to use. Physically, smaller grid point values of  $q_c$  and particularly  $N_c$  typically correspond to broken cloud fields. Thus, we produce two simple, piecewise linear curves relating the shape parameters to the model gridpoint variable values, as shown in Figure 2.

### 3. APPLICATION IN A REGIONAL FORECAST MODEL

COAMPS was run over the California coastal region for a 24 hour period beginning at 00 UTC on 25 July 1997. We present results from the control experiment (without the PDF formulation) and then with the implementation of simple sub-grid statistics described in Section 2. Figure 3 shows this date to exhibit typical summertime stratocumulus features. The cloud system is spatially extensive and exhibits a wide array of inhomogeneity. Near the coast are unbroken stratus, and the boundary layer appears to transition to a more convective regime further to the west, eventually becoming dominated by closed cellular convective elements.

The nested grid configuration, with domains of 18, 6, and 2 km in horizontal grid spacing, is shown in Figure 4. The fine mesh was located a significant distance from the coast to avoid the influence of topographic forcing. The vertical grid spacing is stretched from 10 m near the

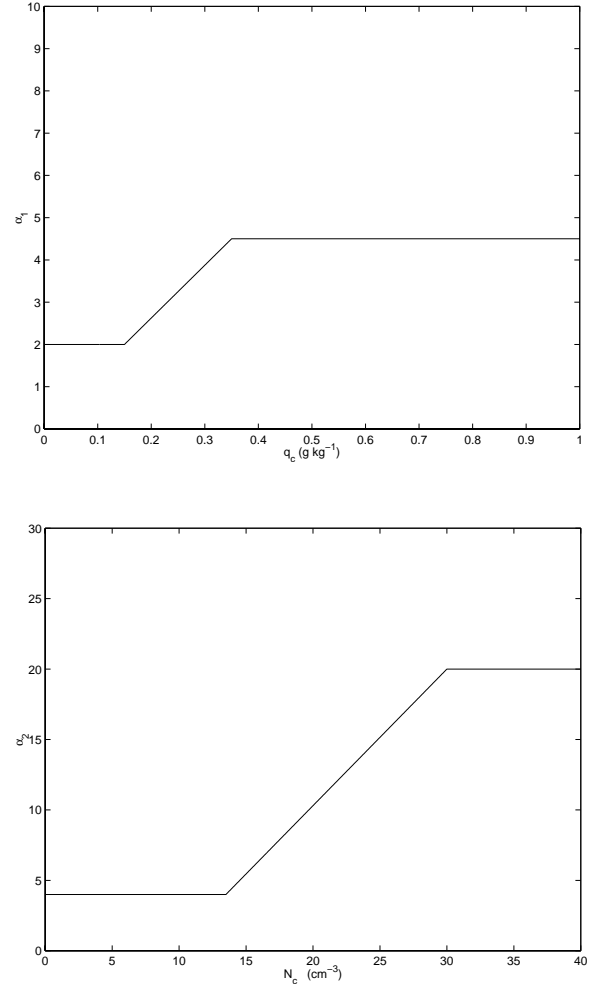


Figure 2. Closure curves derived from LES data for the shape parameters  $\alpha_1$  and  $\alpha_2$ , relating them to grid point values of the cloud variables.

surface to nearly 800 m at the model top. Two 12 h COAMPS simulations using the operational microphysics scheme serve as a preforecast in order to obtain a reasonable boundary layer thermodynamic and cloud field structure. For the 24 hour model simulation, the KK bulk drizzle scheme was used, assuming an initial CCN concentration of  $45.0 \text{ cm}^{-3}$ . This value, representative of a relatively clean air mass, is consistent with the northwesterly flow pattern on 25 July and was chosen to ensure the production of significant drizzle with the hope that breakup of the cloud field would be produced. CCN boundary conditions are fixed at the initial value, and in-situ sources are neglected.

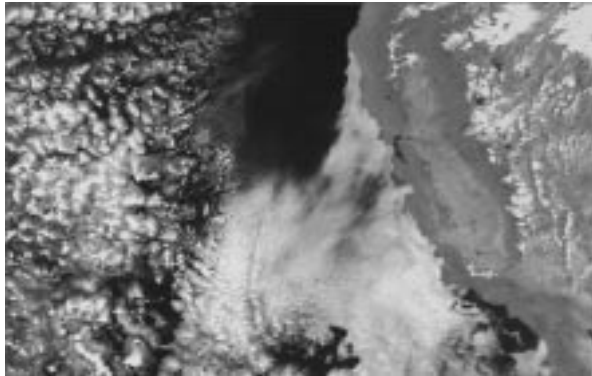


Figure 3. Multi-band AVHRR imagery, a composite of visible and infrared bands, for 1743 UTC 25 July 1997.

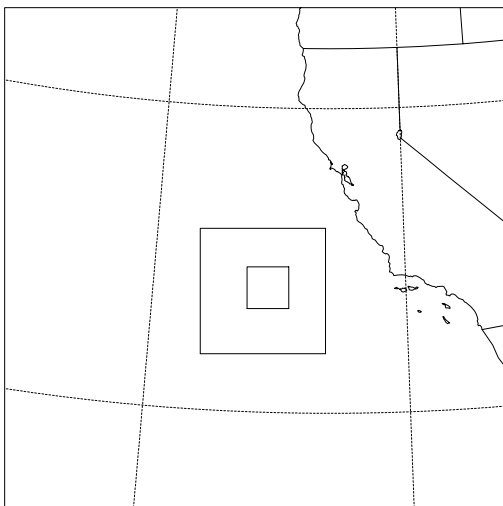


Figure 4. COAMPS domain configuration for coarse, medium, and fine mesh grids (18 km, 6 km, and 2 km, respectively) for the 25 July 1997 simulations.

Liquid water path (LWP) over the 2 km mesh at 18 UTC 25 July 1997 for the control experiment is shown in

Figure 5. Wind barbs indicate northwesterly flow which sets up a quasi-steady transition from unbroken stratocumulus to a boundary layer cumulus regime. Drizzle results in a marked decrease of liquid water content over time, and the resulting stratification suppresses buoyant production of turbulent kinetic energy.

The process of cloud breakup is best thought of in the Lagrangian manner of a parcel entering the domain, moving to the southeast, and undergoing the transition. The boundary layer in the unbroken stratocumulus is initially well mixed, but drizzle produces cooling and moistening throughout the depth of the subcloud layer, causing the boundary layer to become more stable and the cloud layer to decouple from the subcloud layer. Water vapor from the air-ocean interface pools in the surface layer and eventually a condition of potential instability develops, which is realized by cumulus that span much of the depth of the boundary layer. This transition has been documented to occur in LES simulations (Stevens et al. 1998; Khairoutdinov and Kogan 2000) but little prior work has been performed to capture this feature in mesoscale models. Interpretation of the boundary layer cumulus regimes produced in the simulation are complicated by the fact that, nearly all of the vertical circulation in the stratocumulus mode is parameterized, while significant resolved motions are present in the convective regime.

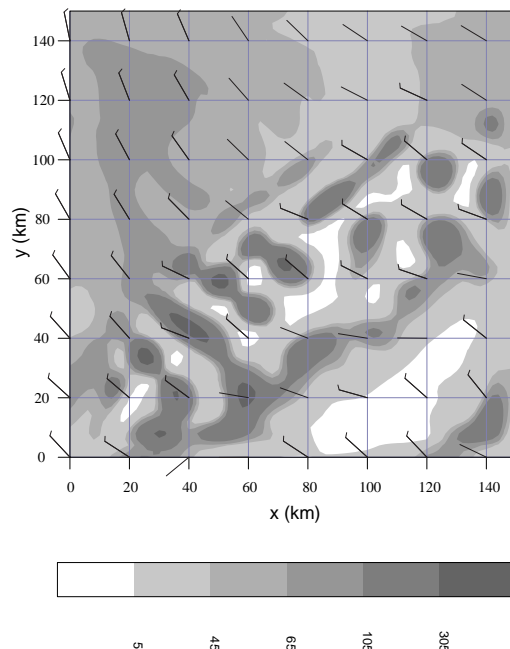


Figure 5. 18 UTC 25 July 1997 LWP ( $\text{g m}^{-2}$ ) over the 2 km mesh for the control experiment.

Figure 6 shows the LWP from a sensitivity experiment that was run using the PDF implementation outlined in Section 2. Including information about sub-grid

variability for the 2 km mesh results in increased auto-conversion rates that lead to enhanced drizzle production and a reduction in liquid water path. Stronger drizzle in this case ultimately leads to a more robust convective mode that acts in the model as a positive feedback on cloud breakup, since the subsiding air outside the cumulus tries to dissipate the cloud.

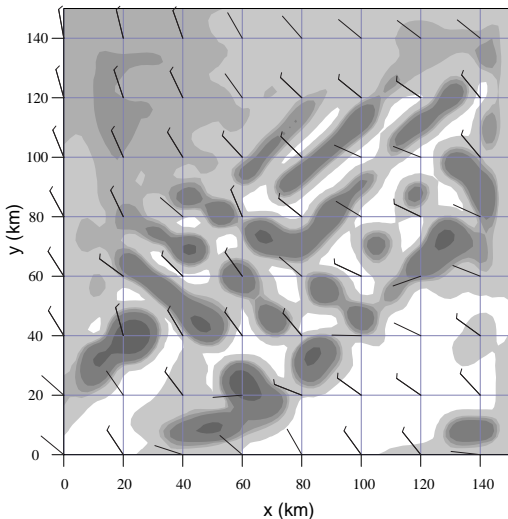


Figure 6. 18 UTC 25 July 1997 LWP ( $\text{g m}^{-2}$ ) over the 2 km mesh for the PDF sensitivity experiment. Shading is the same as in Figure 5.

Enhanced cloud breakup is more obvious when looking at the evolution of cloud fraction. Figure 7 shows that cloud breakup in the PDF experiment is more significant ( $\text{CF} = 0.78$ ) than in the control experiment, which assumes sub-grid homogeneity ( $\text{CF} = 0.93$ ). The spatial plots of LWP are from a time (18 UTC) just before the minimum in cloud fraction. During local afternoon, when the absorption of solar radiation tends to stabilize the cloud layer, the transition dissipates and the cloud field tends to become less broken.

## CONCLUSIONS

Including a simple implementation of sub-grid variability in COAMPS produced enhanced drizzle, increased depletion of cloud water, and a reduced cloud fraction compared to the control case. A treatment of sub-grid inhomogeneity requires a knowledge of cloud variability (statistics) inside a mesoscale grid volume for the particular cloud and atmospheric regime being simulated. These PDFs can be obtained from LES simulations or high resolution observational platforms such as the ARM Millimeter Wave Cloud Radar. As is the case in

any parameterization, these sub-grid statistics (PDFs) must be related to the large scale model variables.

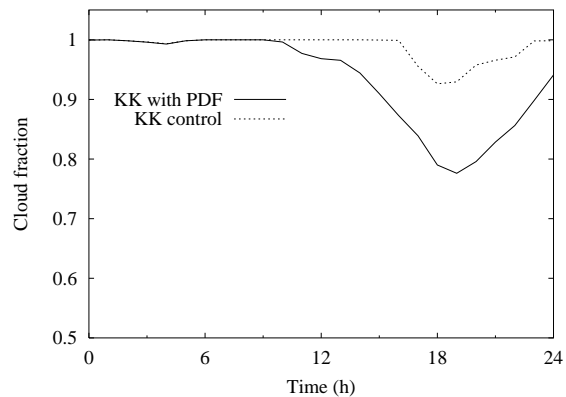


Figure 7. Cloud fraction for the KK control and PDF implementation experiments over the 2 km mesh.

## ACKNOWLEDGEMENTS

This research was supported by the Environmental Sciences Division of the U. S. Department of Energy (through Battelle PNR Contract 144880-A-Q1 to the Cooperative Institute for Mesoscale Meteorological Studies) as part of the Atmospheric Radiation Measurement Program, and by ONR N00014-96-1-0687 and N00014-96-1-1112. Dr. Arulmani supplied the AVHRR imagery.

## REFERENCES

- Cahalan, R. F., W. Ridgway, W. J. Wiscombe, and T. L. Bell, 1994: The albedo of fractal stratocumulus clouds, *J. Atmos. Sci.*, **51**, 2434-2455.
- Hodur, R. M., 1997: The Naval Research Laboratory's Coupled Ocean/Atmosphere Mesoscale Prediction System (COAMPS). *Mon. Wea. Rev.*, **125**, 1414-1430.
- Khairoutdinov, M., and Y. L. Kogan, 2000: A new cloud physics parameterization for large-eddy simulation models of marine stratocumulus. *Mon. Wea. Rev.*, **128**, 229-243.
- Kogan, Y. L., 1998: Parameterization of cloud physics processes in mesoscale models of stratocumulus cloud layers. *AMS Conference on Cloud Physics*, 17-21 August 1998, Everett, Washington.
- Pincus, R., and S. A. Klein, 2000: Unresolved spatial variability and microphysical process rates in large-scale models. *J. Geophys. Res.*, **105**, 27059-27065.
- Stevens, B. W. R. Cotton, G. Feingold, and C.-H. Moeng, 1998: Large-eddy simulations of strongly precipitating, shallow, stratocumulus-topped boundary layers. *J. Atmos. Sci.*, **55**, 3616-3637.